THE ASTROPHYSICAL JOURNAL, 356: L35–L38, 1990 June 20

THE EXTENDED MEDIUM SENSITIVITY SURVEY DISTANT CLUSTER SAMPLE: X-RAY COSMOLOGICAL EVOLUTION[1]

I. M. GIOIA,[2,3] J. P. HENRY,[4] T. MACCACARO,[2,5] S. L. MORRIS,[6] J. T. STOCKE,[7] AND A. WOLTER[2]

Received 1990 February 19; accepted 1990 April 4

ABSTRACT

The X-ray luminosity function of clusters of galaxies is determined at different cosmic epochs using data from the *Einstein Observatory* Extended Medium Sensitivity Survey. The sample consists of 67 X-ray–selected clusters that have been grouped in three redshift shells. Evolution is detected in the X-ray properties of clusters. The present volume density of high-luminosity clusters is found to be *greater* than it was in the past. Given the still limited data set, this result should be regarded as preliminary. It can be interpreted as the consequence of either *luminosity* evolution or modest *density* evolution.

Subject headings: galaxies: clustering — galaxies: evolution — luminosity function — X-rays: general

I. INTRODUCTION

The study of distant clusters of galaxies provides important information on their formation and evolution. Investigations of the X-ray evolution have almost always proceeded by making observations of clusters of galaxies selected in the optical (Henry *et al.* 1982; Henry and Lavery 1984). There is currently little evidence for evolution in X-ray luminosity or temperature for distant optically selected clusters. Surprisingly, for the only two distant systems studied in detail, the cluster 0016+16 at $z = 0.541$ (White, Silk, and Henry 1981) and the cluster around 3C 295 at $z = 0.461$ (Henry and Henriksen 1986), the X-ray properties were found to be similar to those of nearer rich clusters. However, these apparent similarities between distant and nearby systems might be primarily due to a selection effect. Since distant clusters selected optically are chosen because they are especially rich, these clusters may be among the few which have already undergone a considerable amount of dynamical evolution. It is almost impossible to avoid or quantify biases in optically selected samples because they are chosen by eye. Even investigators who presently make catalogs by scanning plates and who select the galaxies and clusters by using rigorous algorithms are faced with the problem of contamination by foreground galaxies and stars.

X-ray selection does not have these biases, even though different selection effects are present. There may be a preference for the detection of high surface brightness systems as well as clusters with deep potential wells. Since the vast majority of the clusters known today have been selected in the optical, it is vital to investigate the properties of a cluster sample extracted from an X-ray survey for a different approach to the understanding of cluster formation and evolution. A Hubble constant $H_0 = 50$ km s^{-1} Mpc^{-1} and a Friedmann universe with a deceleration parameter $q_0 = 0$ are assumed throughout this *Letter*.

II. THE SAMPLE

The sample of clusters of galaxies used in this study is extracted from the *Einstein* Extended Medium Sensitivity Survey (EMSS). A detailed description of the survey sources, the selection criteria, the detection algorithm, the computation of the X-ray flux, and other parameters is given in Gioia *et al.* (1990). We recall here that the EMSS is a flux-limited sample consisting of 835 sources serendipitously detected in Imaging Proportional Counter (IPC) fields at high Galactic latitude, with limiting sensitivities ranging from 5×10^{-14} to 3×10^{-12} ergs cm^{-2} s^{-1} in the 0.3–3.5 keV energy band. A detailed discussion of the identifications, as well as presentation of finding charts and spectral and photometric data, will be presented elsewhere (Stocke *et al.* 1990; Maccacaro *et al.* 1990). For the purpose of this study we have considered only sources with declination greater than −40° (accessible from Mauna Kea) and flux greater than 1.5×10^{-13} ergs cm^{-2} s^{-1} in a $2'.4 \times 2'.4$ detection cell (to reduce the number of still unidentified sources). Adopting these criteria, the survey contains 733 sources and is 97% identified. There are 93 sources identified with clusters of galaxies. Since most nearby clusters were observed as a target of IPC observations, they were not available to be detected serendipitously by the EMSS, so this sample is not complete at the low end of the redshift distribution. For this study we have chosen to use only those clusters in our sample with a redshift greater than 0.14. This value roughly corresponds to Abell distance classes 5–6. Since the majority of the Abell clusters chosen as the target of the IPC observations belong to distance class 3 or less, we feel comfortable in using the value of 0.14 as a lower limit in redshift. The resulting sample contains 67 objects. It is the most numerous sample of distant clusters of galaxies extracted from a flux limited survey of "faint" X-ray sources, i.e., the sample is defined exclusively by its X-ray properties. The precise knowledge of the area of sky searched for X-ray sources and of the limiting sensitivity pertaining to each area allows us to derive the cluster X-ray luminosity function. In the redshift range $0.14 \leq z < 0.20$, there are 20 clusters of which only four are in the Abell catalog. The X-ray luminosities of objects in this shell are all greater than 10^{44} ergs s^{-1}. Since clusters with this luminosity are almost exclusively Abell clusters at lower redshift, it is somewhat surprising that we find so few of them. Although our clusters are mostly *not* Abell clusters, it is prema-

---

[1] This *Letter* uses data obtained at the Multiple Mirror Telescope Observatory (MMTO), which is operated jointly by the University of Arizona and the Smithsonian Institution, and at the University of Hawaii 2.2 m Telescope.

[2] Harvard-Smithsonian Center for Astrophysics.

[3] Istituto di Radioastronomia del CNR, Bologna.

[4] Institute for Astronomy, University of Hawaii, Honolulu.

[5] Osservatorio Astronomico di Bologna.

[6] The Observatories of the Carnegie Institute of Washington.

[7] Center for Astrophysics and Space Astronomy, Boulder.

ture to discuss the implications of these results on the completeness of the Abell catalog until more optical work is done on our clusters.

Even though the EMSS is statistically well defined, there are still a number of effects in the data which must be taken into account. These effects are absorption by the Milky Way, the different redshifts of the sources, the different sky coverage for different flux limits, and the correction for lost flux due to the finite source size (the EMSS uses a detection cell of 2′.4 × 2′.4). We discuss the corrections we have applied to take into account each of these effects on our data. We note here that the EMSS uses the so-called M-DETECT algorithm to find sources. In this method the background is computed from a global map of the detector so that sources are not lost because their extended flux distribution mistakenly increases the apparent background around them (see Gioia *et al.* 1990 for a detailed discussion).

The flux from each source has been corrected for absorption using the neutral hydrogen values from the survey of Stark *et al.* (1984). Most of the sky was observed through a small range of N_H which results in a negligible bias (see Zamorani *et al.* 1988; Maccacaro *et al.* 1988). *K*-corrections are small for our sample. Assuming a Raymond-Smith spectrum at a redshift of 0.5, the correction is always within 15% of unity for temperatures between 2 and 10 keV (R. Burg 1989, private communication) and is less at smaller redshifts. Therefore, for simplicity we used *K*-corrections calculated assuming a power-law spectrum with energy index of 0.5, which roughly approximates a 6 keV thermal spectrum in our 0.3–3.5 keV energy band. The sky coverage north of −40° declination has been calculated adopting the same spectrum and procedures used to determine the flux of the clusters, i.e., using only the counts in the detection cell without applying any correction for the point response function.

The largest correction is for the effect of the finite size of the X-ray emisssion in clusters. This correction will be used in two places: first, to calculate the true luminosity of a cluster when only its detection cell flux and redshift are known, and second, to determine the amount of flux that would appear in the detection cell at different redshifts during the calculation of the maximum observable redshift (see § III) in the derivation of the luminosity function. We adopt the β model for the cluster brightness, that is,

$$I(\theta) = \frac{I_0}{[1 + (\theta/\theta_0)^2]^{(3\beta - 1/2)}} .$$

From Jones and Forman (1984), we adopt $\beta = \frac{2}{3}$. Then integrating over the square detection cell between 0 and θ_D we obtain the observed flux:

$$F_{\rm obs} = 4 \int_0^{\theta_D} d\theta_x \int_0^{\theta_D} d\theta_y I(\theta) ,$$

where θ_D is the angular half-size of the detection cell (1′.2). The integration gives

$$F_{\rm obs} = 2\pi I_0 \theta_0{}^2 f\left(\frac{\theta_D}{\theta_0}\right) ,$$

where

$$f\left(\frac{\theta_D}{\theta_0}\right) = \frac{1}{2} + \frac{1}{\pi} \sin^{-1}\left[\frac{(\theta_D{}^2/\theta_0{}^2 - 1)^2 - 2}{(\theta_D{}^2/\theta_0{}^2 + 1)^2}\right] \qquad (1)$$

is the fraction of the total flux in the detection cell. We determine θ_0 using the 18 Piccinotti *et al.* (1982) clusters (*HEAO 1* A-2 experiment) which have IPC imaging data and which are not so large that they extend beyond the IPC ribs. This sample is X-ray selected and seems to be the most comparable with our sample. For these 18 clusters, we calculate the average fraction of the total flux (as determined by Piccinotti *et al.*) which is detected by the EMSS detection cell if each cluster were at a fiducial redshift. The arbitrary fiducial redshift was chosen to be 0.35 which gives $D_A \times \theta_D = 0.5$ Mpc, where D_A is the angular diameter distance. At this redshift, the average fraction of flux of the Piccinotti *et al.* objects that would be in the detection cell is equal to 0.43 with a large dispersion ($\sigma = 0.2$). No obvious dependence is found between this fraction and the X-ray luminosity of the clusters. From equation (1), $D_A \times \theta_0 = 0.37$ Mpc. Equation (1) with this value of θ_0 is used to correct the observed luminosity to the total luminosity. The redshift dependence of I_0 and θ_0 are

$$I_0(z) = \frac{I_0(1 + z_{\rm obs})^4}{(1 + z)^4}$$

and

$$\theta_0(z) = \frac{\theta_0 D_A(z_{\rm obs})}{D_A(z)} ,$$

where $z_{\rm obs}$ is the redshift of the cluster. We assume that θ_0 and β do not evolve with redshift. Performing a similar integral over the detection cell for the cluster at an arbitrary redshift gives

$$F(z) = F_{\rm obs} \frac{D_L{}^2(z_{\rm obs})}{D_L{}^2(z)} \frac{f[D_A(z)\theta_D/D_A \theta_0]}{f[D_A(z_{\rm obs})\theta_D/D_A \theta_0]} , \qquad (2)$$

where D_L is the luminosity distance and $z_{\rm obs}$ is the observed redshift of the cluster. This expression is used in the calculation of the maximum redshift at which a given object could have been detected. It reduces to the point source result in the limit that the size of the detection cell is much larger than that of the cluster.

III. THE X-RAY LUMINOSITY FUNCTION

In this section we derive and discuss the X-ray luminosity function (XLF) for clusters of galaxies computed in three different redshift shells defined by $z_{\rm low}$ and $z_{\rm high}$. A nonparametric representation of the XLF is first obtained using the $1/V_a$ method of Avni and Bahcall (1980), a generalization of the $1/V_{\rm max}$ method (Schmidt 1968) when several complete samples are analyzed. For each cluster falling in one of the three $z_{\rm low}$–$z_{\rm high}$ shells defined later, we computed the maximum redshift ($z_{\rm max}$) at which the source could have been seen taking into account the solid angle observed at different limiting sensitivities. The maximum volume in which the cluster could have been detected depends on the redshift of the shell under consideration, the luminosity of the cluster, and the sky coverage of the EMSS. The search volume for a given cluster, V_a, is the sum of all volumes lying between the minimum redshift $z_{\rm low}$ of the shell under consideration and the lesser of the maximum shell redshift $z_{\rm high}$ or the maximum redshift $z_{\rm max}$ at which the source could have been seen for each different sensitivity limit. The individual contributions have been binned by log lumin-

1990ApJ...356L..35G

osity to create the differential XLF, $N(L)$, integrated in independent bins 0.3 wide in $\Delta \log L$. For each bin we have

$$N(L) = \sum_{j=1}^{n} \frac{1}{V_{a,j}\Delta L},$$

where n is the number of objects in that bin. The results are shown in Figure 1, where the three panels give the XLFs in redshift shells as indicated. There are 20 clusters with redshift $0.14 \le z < 0.20$, 26 clusters with redshift $0.20 \le z < 0.30$, and 21 clusters with redshift $0.30 \le z < 0.60$. The 1 σ error bars associated with each bin are determined from the number of objects contributing to that bin and have been computed using Poisson statistics (Regener 1951).

We then consider a parametric representation of the luminosity function of the form

$$\frac{dN(L_{44})}{dL_{44}} = KL_{44}{}^{-\alpha},$$

where L_{44} is the X-ray luminosity in units of 10^{44} ergs s^{-1} and K is the normalization coefficient expressed in units of Mpc$^{-3}L_{44}{}^{-1}$. The maximum likelihood method (see Murdoch, Crawford, and Jauncey 1973, and references therein) has been applied to the unbinned data to estimate the best-fit slopes which are given in Table 1 with their associated 1 σ errors. The fits have been computed in each redshift range between the minimum observable luminosity $L_{\min}$ and the infinite luminosity.

The normalization coefficient K has been computed by requiring that the number of expected objects equals the number of observed objects. Errors on K have been determined by letting α assume the 1 σ extremes in each case. A steepening of the slope is observed at higher redshifts. This change is best seen in Figure 2 where the differential XLFs for clusters in the lowest shell ($0.14 \le z < 0.20$) and in the highest shell ($0.30 \le z < 0.60$) are plotted. The difference between the two slopes is significant at the 3 σ confidence level.

We note that no cluster with $\log L_x > 45.2$ has been detected at low redshift ($0.14 \le z < 0.20$). Clearly these clusters, which have been detected at higher redshift, could have been detected at lower redshift. However the available volume in the low redshift shell is much smaller than the volume in the higher redshift shells. Only one cluster is expected in the bin centered at $\log L_x = 45.35$. Thus the absence of $\log L_x > 45.2$ clusters in the low-z shell is not significant and is not necessarily indicative of a break in the XLF of low-redshift clusters. It is of interest to compare our lowest redshift XLF with that of Piccinotti *et al.* (1982) even though their sample was at a lower redshift and in a different energy band. The two slopes agree (2.09 vs. 2.15) within the errors. With the same 6 keV thermal spectrum we used previously to compute our fluxes, we find that the Piccinotti normalization, converted from their 2–10 keV band to our 0.3–3.5 keV, is 2.1 ± 1.6 times smaller than ours. That is we essentially agree within the errors.

TABLE 1

PARAMETRIC REPRESENTATION OF THE CLUSTER X-RAY LUMINOSITY FUNCTION

z	α	K(Mpc^{-3} $L_{44}{}^{-1}$)	$\log L_{\min}$
0.14–0.20.........	2.09 ± 0.20	$(7.19 \pm 0.58) \times 10^{-7}$	42.90
0.20–0.30.........	2.63 ± 0.22	$(10.8 \pm 1.56) \times 10^{-7}$	43.30
0.30–0.60.........	3.09 ± 0.27	$(12.2 \pm 4.46) \times 10^{-7}$	43.80

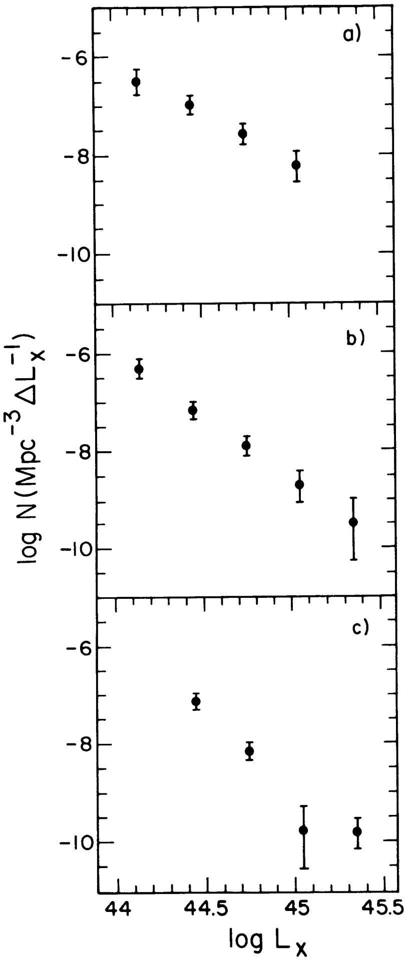

FIG. 1.—The differential luminosity functions of clusters in the three redshift shells: (a) $0.14 \le z < 0.20$, (b) $0.20 \le z < 0.30$, and (c) $0.30 \le z < 0.60$.

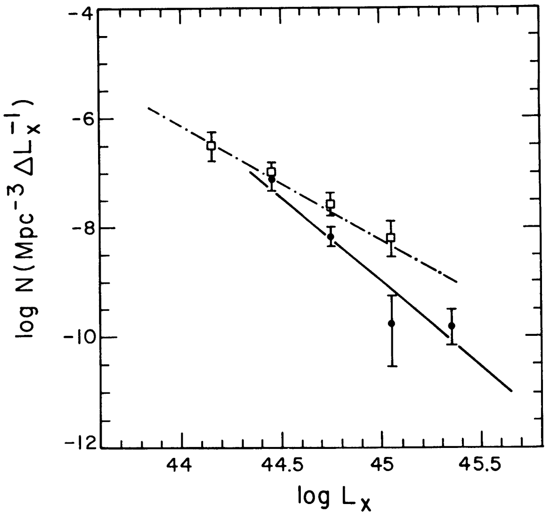

FIG. 2.—A comparison of the differential luminosity functions for the lowest (*open squares*) and the highest (*filled dots*) redshift shells. The straight lines represent maximum likelihood fits to the individual unbinned data.

IV. DISCUSSION

We believe we have the first convincing evidence for evolution in the X-ray properties of clusters, even if our result is significant only at the 3 σ level. Note that the slopes are independent of the correction applied for the flux lost outside of the detection cell because all the sources in each shell are at approximately the same redshift. The XLF which characterizes high-redshift clusters ($0.30 \leq z < 0.60$) is significantly steeper than the XLF of low-redshift clusters ($0.14 \leq z < 0.20$). This trend is supported by the intermediate XLF ($0.20 \leq z < 0.30$). We have assumed that θ_0 does not evolve. If, however, the core radius decreases with increasing redshift, as would be expected in a hierarchical scenario, then we would make a smaller correction for the flux lost outside the detection cell, would have fewer high-luminosity clusters, and would find even stronger evolution than we do.

The luminosity range covered by our data is rather limited and prevents a detailed analysis of the shape and kind of cosmological evolution. Furthermore, there are still 19 sources unidentified which could modify the results presented in this *Letter*. However evolution seems present only at high luminosities ($\log L_x \geq 44.7$). At lower luminosities ($44.2 \leq \log L_x < 44.7$), no significant difference exists as a function of redshift. This behavior is suggestive of a *luminosity-dependent* evolution such that the volume density of high-luminosity clusters ($\log L_x \geq 44.7$) is higher at the present epoch than at epochs corresponding to redshifts of about 0.5. The volume density of low-luminosity clusters has remained unchanged. Presumably our power-law characterization of the data could be naive and a luminosity function with a break analogous to a Schechter function could be more appropriate. In this case, the different slopes observed could be the result of either *luminosity evolution*, with the break shifted to a higher luminosity for the lower redshift clusters, or a modest *density evolution*. In the latter case, the apparent change in slope would result because the high-redshift sample, with intrinsically more luminous clusters in the mean, has more objects drawn from above the break relative to the low-redshift samples.

The basic conclusion is that there is good evidence for a *difference between the X-ray luminosity function at high and low redshift*. This difference goes in the *opposite sense* to that anticipated by Kaiser (1986) who predicted density evolution in the sense that there would have been a higher volume density of X-ray clusters in the past. By contrast, the evidence for evolution we have found, that is fewer clusters in the past, is in the *same sense* as anticipated by Perrenod (1980) (see also Cavaliere and Colafrancesco 1988). After this *Letter* had been submitted we received a preprint from Edge *et al.* (1990) who found a similar result from an independent data set.

Finally, based on a study of the effects of cooling flows on the EMSS X-ray source counts of clusters of galaxies, Pesce *et al.* (1990) suggested that in all high-z EMSS clusters, there are significant cooling flows. An optical study of these same clusters based on Hα imaging, initiated by Donahue *et al.* (1990), does not find a larger percentage of $z \geq 0.3$ clusters with strong extended Hα emission compared to lower z clusters. Certainly the EMSS detects cooling flow clusters more easily, though the fraction among our cluster sample may be somewhat smaller than Pesce *et al.* suggested.

We would like to thank R. Giacconi and R. Burg for many interesting discussions when this work was at an early stage of preparation and G. Zamorani for many helpful suggestions and comments. This work has received partial financial support from NASA contract NAS8-30751, NASA grants NAG8-738 and NAG5-1256, NSF grant AST 8715983, and from the Smithsonian Institution Scholarly Studies grants SS48-8-84 and SS88-3-87.

REFERENCES

Avni, Y., and Bahcall, J. N. 1980, *Ap. J.*, **235**, 694.
Cavaliere, A., and Colafrancesco, S. 1988, *Ap. J.*, **331**, 660.
Donahue, M. E., Stocke, J. S., Shull, J. M., and Gioia, I. M. 1990, *Bull. AAS*, in press.
Edge, A. C., Stewart, G. C., Fabian, A. C., and Arnaud, K. A. 1990, *M.N.R.A.S.*, submitted.
Gioia, I. M., Maccacaro, T., Schild, R. E., Wolter, A., Stocke, J. S., Morris, S. L., and Henry, J. P. 1990, *Ap. J. Suppl.*, **72**, 567.
Henry, J. P., and Henriksen, M. J. 1986, *Ap. J.*, **301**, 689.
Henry, J. P., and Lavery, R. J. 1984, *Ap. J.*, **280**, 1.
Henry, J. P., Soltan, A., Briel, U., and Gunn, J. E. 1982, *Ap. J.*, **262**, 1.
Jones, C. J., and Forman, W. R. 1984, *Ap. J.*, **276**, 38.
Kaiser, N. 1986, *M.N.R.A.S.*, **222**, 323.
Maccacaro, T., Gioia, I. M., Wolter, A., Zamorani, G., and Stocke, J. T. 1988, *Ap. J.*, **326**, 680.
Maccacaro, T., *et al.* 1990, in preparation.
Murdoch, H. S., Crawford, D. E., and Jauncey, D. L. 1973, *Ap. J.*, **183**, 1.
Perrenod, S. C. 1980, *Ap. J.*, **236**, 373.
Pesce, J. E., Fabian, A. C., Edge, A. C., and Johnstone, R. M. 1990, *M.N.R.A.S.*, in press.
Piccinotti, G., Mushotzky, R. F., Boldt, E. A., Holt, S. S., Marshall, F. E., Serlemitsos, P. J., and Shafer, R. A. 1982, *Ap. J.*, **253**, 485.
Regener, V. H. 1951, *Phys. Rev.*, **84**, 161L.
Schmidt, M. 1968, *Ap. J.*, **151**, 393.
Stark, A. A., Heiles, C., Bally, J., and Limke, R. 1984, Bell Labs, privately distributed magnetic tape.
Stocke, J. T., *et al.* 1990, in preparation.
White, S. D. M., Silk, J., and Henry, J. P. 1981, *Ap. J. (Letters)*, **251**, L65.
Zamorani, G., Gioia, I. M., Maccacaro, T., and Wolter, A. 1988, *Astr. Ap.*, **196**, 39.

I. M. Gioia, T. Maccacaro, and A. Wolter: Harvard-Smithsonian Center for Astrophysics, 60 Garden Street, Cambridge, MA 02138

J. P. Henry: Institute for Astronomy, University of Hawaii, 2680 Woodlawn Drive, Honolulu, HI 96822

S. L. Morris: The Observatories of the Carnegie Institute of Washington, 813 Santa Barbara Street, Pasadena, CA 91101

J. T. Stocke: Center for Astrophysics and Space Astronomy, University of Colorado, Campus Box 391, Boulder, CO 80309